INSTITUTE OF PHYSICS PUBLISHING and INTERNATIONAL ATOMIC ENERGY AGENCY NUCLEAR FUSION

Nucl. Fusion **43** (2003) 594–605 PII: S0029-5515(03)64085-8

Study of thermonuclear Alfvén instabilities in next step burning plasma proposals

N.N. Gorelenkov[1], H.L. Berk[2], R. Budny[1], C.Z. Cheng[1], G.-Y. Fu[1] W.W. Heidbrink[3], G.J. Kramer[1], D. Meade[1] and R. Nazikian[1]

[1] Princeton Plasma Physics Laboratory, P.O. Box 451, Princeton, NJ 08543-0451, USA
[2] IFS, Austin, Texas, USA
[3] University of California, Irvine, California 92697, USA

Received 25 September 2002, accepted for publication 20 May 2003
Published 2 July 2003
Online at stacks.iop.org/NF/43/594

Abstract
The stability of α-particle driven shear Alfvén eigenmodes (AE) for nominal burning plasma (BP) parameters in the proposed international tokamak experimental reactor (ITER), fusion ignition research experiment (FIRE) and IGNITOR tokamaks is studied. JET plasma, where fusion αs were generated in tritium experiments, is also studied to compare the numerical predictions with the existing experiments. An analytic assessment of toroidal AE (TAE) stability is first presented, where the α-particle β due to the fusion reaction rate and electron drag is simply and accurately estimated in plasmas with central temperature in the range of 7–20 keV. In this assessment the hot particle drive is balanced against ion-Landau damping of the background deuterons, and electron collision effects and stability boundaries are determined. Then two numerical studies of AE instability are presented. In one, the HIgh-n STability (HINST) code is used to predict the instabilities of low and moderately high frequency Alfvén modes. HINST computes the non-perturbative solutions of the AE including effects of ion finite Larmor radius, orbit width, trapped electrons etc. The stability calculations are repeated using the global code NOVAK. We show that for these plasmas the spectrum of the least stable AE modes is at medium-/high-n numbers. In HINST, TAEs are locally unstable due to the α pressure gradient in all the devices under consideration except IGNITOR. However, NOVAK calculations show that the global mode structure enhances the damping mechanisms and produces stability for the nominal FIRE proposal and near-marginal stability for the nominal ITER proposal. NBI ions produce a strong stabilizing effect for JET. However, in ITER, the beam energies needed to penetrate to the core must be high ($\sim$1 MeV) so that a diamagnetic drift frequency comparable to that of α-particles is produced by the beam ions which induces a destabilizing effect. A serious question remains whether the perturbation theory used in NOVAK overestimates the stability predictions, so that it is premature to conclude that the nominal operation of all three BP proposals without neutral beam injection are stable (or marginally stable) to AEs.

PACS numbers: 52.35.Bj, 52.55.Pi

1. Introduction

In a fusion producing deuterium–tritium (D–T) tokamak plasma the 3.5 MeV α-particles must be trapped by the magnetic field so that their energy can be transferred, primarily through electron drag, to the background plasma. It is the purpose of burning plasma (BP) experiments to demonstrate that this method of self-heating will be the dominant method of heating of a plasma that is producing fusion energy. However, the α-particle partial pressure is significant and a physical issue arises whether this pressure is capable of inducing collective behavior that may cause the premature loss of α-particles. Should this be the case, two major problems may arise: (i) it may become difficult to sustain the plasma parameters close to the ignition and (ii) the fluxes of energetic α-particles ($\sim$3.5 MeV) to the first wall of the experiment can cause severe wall damage.

Indeed, it has been demonstrated in present day (PD) experiments that the collective effects induced from energetic particles can result in premature α-particle loss. However, it is difficult to obtain a comprehensive extrapolation of the results of PD experiments to what would be expected for BP experiments. The fast particle distribution functions are often quite different. In PD experiments, the energetic particle distribution are anisotropic whereas in a BP experiment the distribution function of fusion α-particles is isotropic.

In addition, in a BP experiment the machine size to orbit width will be significantly larger and the spectrum (and number) of unstable modes is likely to be broader in BP compared with PD experiments. Thus, even with continued study in PD experiments, extrapolation to reliable predictions for BP experiments may remain uncertain without actually performing these BP experiments.

It is generally believed that the toroidal Alfvèn eigenmodes (TAEs) [1–4] destabilized by fast ions, are the plasma waves most likely to cause significant difficulties for the containment of energetic α-particles in fusion energy generating tokamak experiments. It has been experimentally established that in presence of a strong enough energetic particle energy density these modes will induce large losses of fast particles, though it is also known that there is a wide variety of conditions where these modes are stable or when unstable, do not induce anomalous loss. Experimental reviews of TAEs and other relevant issues of fast particle physics can be found in [5, 6]. The purpose of this paper is to determine whether linear instability to the TAEs is expected under BP conditions. In particular, we study the TAE stability for the three proposed BP experiments now being considered by the fusion research community, international tokamak experimental reactor (ITER)-FEAT [7], fusion ignition research experiment (FIRE) [8] and IGNITOR [9]. By and large, we will numerically study the stability for the proposed nominal operating conditions. With the use of analytic estimates some extrapolation is possible to other temperature regimes of operation.

We will present three types of stability analyses. The first is based on an analytic analysis where we estimate the α-particle drive and compare it with the two damping mechanisms that are expected to dominate for most of the parameters relevant to the machines being proposed and their modes of excitation. The analytic study is based on simplified scaling, assuming that the base TAE structure is a 'couplet' formed at $q(r) = (m + 1/2)/n$ by two poloidal mode numbers with values m and $m+1$, can be used to characterize the stability of the global mode structure even though a realistic mode structure is generally more complex than the assumed local structure. We will see that this analysis correlates favourably with detailed numerical calculations. Therefore, the analytic analysis gives a guide as to how the stability conditions change as parameters of the proposed experiment are varied from the nominal machine parameters that the numerical studies concentrate upon.

The second method is a numerical study using the HIgh-n toroidal STability (HINST) code [10], which has been improved to describe the effect of finite orbit width and the finite Larmor radius (FLR) of the energetic particles in realistic numerical equilibria. HINST is a high-n ballooning code that can be applied accurately down to moderate n-numbers (e.g. $n \sim 5$). It is limited by being a localized code, and as such does not account for the extended spatial mode structure of TAE modes. However, HINST has the virtue of being a non-perturbative code. As such it can describe the so-called resonant TAE (RTAE) [11] (alternatively called the energetic particle mode (EPM) [12–14]) EPMs that can even arise in MHD continuum. Such modes may be related to experimentally observed beta-induced Alfv́en eigenmodes (BAE) [15]. This was shown with HINST stability analysis for medium-n numbers modes [16, 17]. Another example of the experimental validation of HINST code is the observation of the high-n precursors of the sawtooth crash in TFTR [18] which were explained as R-TAEs with HINST and were found to be in good agreement with the stability analysis [19] (see also the analysis for JT-60U in this reference).

Further, an extremely important damping mechanism, radiation damping, is treated precisely in HINST. Previously, in full machine codes that made extensive studies of TAE instabilities in realistic designed experiments (such as NOVA [20]), radiation damping was only treated perturbatively and in a regime of limited accuracy [21]. This technique apparently under-estimates damping. Other codes, such as CASTOR-K [22] treat radiation damping in a non-perturbative manner, but the instability drive is still treated perturbatively. It should be noted that radiation damping becomes a significant damping mechanism when core ion FLR (as well as electron reactance) effects increases [11,23–25] and becomes a strongly stabilizing effect at $k_\perp \rho_i \sim \sqrt{r/R}$, where $k_\perp$ is the characteristic radial wavenumber of a TAE mode and ρ_i is the bulk ion Larmor radius calculated for ions with thermal velocity $v_T = \sqrt{2T/m}$. This damping mechanism may then compete with the α-particle drive at moderately high toroidal mode numbers n. The fast particle drive reaches a maximum for n-numbers near $nq^2\rho_h/r \simeq 1$, where ρ_h is the fast ion Larmor radius, and then beyond this value decreases with increasing n. Depending on detailed parameters, radiation damping may be a significant damping mechanism near the peak of the α-particle drive. In addition HINST includes in a non-perturbative manner, damping from ion Landau damping, electron collisionality, and electron Landau damping.

The third stability study of the proposed nominal parameters of the BP experiments uses the NOVA and NOVA-K codes. NOVA/NOVA-K codes were successfully used to predict and model medium-n TAE instabilities (their thresholds and frequencies) in D–T experiments on TFTR [26], which were observed in the beam heated plasma [27]. These are basically the same codes that were used to study the TAE stability of plasmas in the original ITER design. These codes are based on a perturbative procedure, where the lowest order mode structure is first found using the ideal MHD NOVA code by neglecting damping and drive sources. Then the NOVA-K code incorporates these sources through a perturbative procedure. At moderate- to high- n's the lowest order mode is often extended over the whole minor radius. When there is no difficulty of exciting the continuum at some radial position, the global structure of the TAE mode is used as a lowest order approximation to the eigenmode.Then the α-particle drive and the numerous damping mechanisms (including a model for radiation damping) is incorporated in a perturbative manner to predict stability. Recently, NOVA/NOVA-K codes were used to explain high-n odd core localized TAEs observed in ICRH JET discharges with good accuracy [28], in which the stability of these modes was critical for their excitation.

It should be noted that there are deficiencies in the procedures used in the NOVA/NOVA-K codes. Frequently, the continuum cannot be avoided and the damping, as well as alteration of mode structure due to the presence of the

continuum, is ignored. The inclusion of the continuum damping may stabilize some of the global low-n modes we predict to be unstable. At higher n-values that are studied in this code, there is a tendency for the TAE modes at a given n-number to be nearly degenerate. This gives rise to the possibility that the basic mode structures may be different than the zeroth order structures that emerge from the code (which often extend through a large fraction of the plasma). Of particular concern is the tendency for strong collisional damping arising from the mode structure at the outer edge of the plasma, to stabilize a mode where the drive is located in the central region of the plasma. A more sophisticated perturbation theory may need to be implemented to determine if TAE modes might localize in regions where the drive dominates. However, for this study we report solely on the predictions of the present set of codes with its present calculational methods.

2. Analytical stability model

2.1. Fast particle TAE drive

To understand the parametric dependence of the drive of TAE modes we use the model that the α-particles are created at $\mathcal{E}_{\alpha 0} = 3.52\,\mathrm{MeV}$ and then slow down due to electron drag. It is adequate to take the α-particle distribution function of the form,

$$f_0(v) \simeq 2^{-5} 3\pi^{-2} \beta_\alpha B^2 \theta \frac{v_{\alpha 0} - v}{\mathcal{E}_{\alpha 0} v^3}$$

with β_α the α-particle β-value, $\theta(x)$ the step function, $v_{\alpha 0}$ the birth speed of the α-particles.

The α-particle drive, γ_α/ω, is in a plateau regime [29–31] for the toroidal mode numbers lying in the range

$$n_{\min} \simeq \frac{r}{R} n_{\max} < n < n_{\max} \simeq \frac{r\omega_{c\alpha}}{q^2 v_A}. \tag{1}$$

The appropriate expression for the growth rate in this plateau regime was obtained in [29, 30]. Comparison of this analytic expression with the numerical calculations in NOVA-K in the limit of a low β when the flux surface has circular cross-section shows quantitative agreement when FLR effects are neglected. The growth rate when the shear s is less than unity (with a factor insensitive to s as it approaches unity) was found to be,

$$\frac{\gamma_\alpha}{\omega} \simeq -\frac{5\pi}{2} q^2 r \frac{\partial \beta_\alpha}{\partial r} x_A (1 - x_A^2), \tag{2}$$

where $x_A = v_A/v_{\alpha 0} < 1$ and in [31] the effect of FLR was found to lower this plateau result by about 20% for core localized TAEs.

2.2. Damping mechanisms

The damping rate dependence on plasma parameters is more complicated and includes TAE energy radiation through the thermal ion FLR effects (as well as comparable electron impedance effects) which leads to a modification of the eigenfunction. Different contributions to damping can be expressed analytically in a limited domain of plasma parameters and are incorporated in the NOVAK study. The radiation damping expression from [21, 25] is very sensitive to plasma parameters, and is difficult to incorporate into a simple expression that is typical for the entire machine. However, frequently, radiation damping is negligible for a low β plasma in which the TAE frequency is located near the centre of the gap so that TAE only weakly interacts with the continuum modes. This also follows from the simulations (see later). Thus, a reasonable estimate of the damping can be obtained by only including the thermal ion Landau damping from deuterons and trapped electron collisional damping, as we will see in section 3.1. The analytic formula for Landau damping of Maxwellian ions [4], which is applicable to the large aspect ratio localized TAE solutions, is:

$$\frac{\gamma_{i\mathrm{Land}}}{\omega} = -\frac{q^2\sigma\sqrt{\pi}\beta_{\mathrm{pc}}}{2(1+\sigma)} x_i^5 \mathrm{e}^{-x_i^2} = -\frac{q^2\sigma\sqrt{\pi}}{18(1+\sigma/4)} x_i^3 \mathrm{e}^{-x_i^2}, \tag{3}$$

where $\sigma = (n_D + n_T)/n_e$ is the plasma ion depletion factor close to unity,

$$x_i = \frac{v_A}{3v_i} \simeq \sqrt{\frac{1+\sigma}{9(1+\sigma/4)\beta_{\mathrm{pc}}}}, \tag{4}$$

β_{pc} is the core plasma β which includes thermal electrons and ions, and $v_i = \sqrt{2T_i/m_i}$ is the ion thermal velocity.

Here, we assumed $x_i \gg 1$, so that in a D–T plasma mixture only deuterium contributes to the damping rate, since its thermal velocity is larger than the tritium one. Note, that in [31] this formula was shown to accurately describe ion Landau damping for core localized TAEs. For simplicity, we assume that there is only one impurity specie with a mass to charge ratio the same as that of deuterium.

The second major damping mechanism considered in this analytic study is the trapped electron collisional damping of TAE modes [32, 33], which becomes dominant in lower temperature/higher density plasmas. The damping can be approximately expressed as [33]

$$\frac{\gamma_e}{\omega} \simeq -\sqrt{\frac{\pi}{2}}\frac{1}{4}\left[I_1\left(\frac{8snq\rho_s}{5r\epsilon}\right)^2 + I_2 q^2 \frac{8\beta_{\mathrm{pc}}}{1+\sigma}\right]\sqrt{\frac{\nu}{\omega}} \times \left[\ln\left(16\sqrt{\frac{\omega\epsilon}{\nu}}\right)\right]^{-3/2}, \tag{5}$$

where we approximate coefficients I_j with good accuracy as follows $I_1 = (0.43 Z_{\mathrm{eff}} + 1.06)$, and $I_2 = (1.03 Z_{\mathrm{eff}} + 2.3)$. For one specie impurity, we have $Z_{\mathrm{eff}} = \sigma + Z_i(1-\sigma)_{|Z_i=6} = 6 - 5\sigma$. The electron collisional frequency is

$$\begin{aligned}\frac{\nu}{\omega} &= \frac{4\pi n_e \mathrm{e}^4 \ln(\Lambda_e)}{\omega m_e^2 v_e^3} \\ &\simeq \frac{2\sqrt{2}\pi}{3}\sqrt{\frac{m_p}{m_e}}\frac{n_e \mathrm{e}^4 \ln(\Lambda_e) q R}{x_i T_e^2} \\ &\simeq 0.145 \frac{R_{[m]} q}{x_i^3} \frac{B^2_{[10\,\mathrm{T}]}}{(1+\sigma/4) T^3_{[10\,\mathrm{keV}]}},\end{aligned} \tag{6}$$

where we assumed that electron Coulomb logarithm equals 20 and the plasma parameter subscripts in square brackets denotes the units to be used. The toroidal mode dependence in equation (5) suggests that for the most unstable mode we should take the lowest n-value that lies within the plateau

regime of the α-particle drive, $n_{\min}$:

$$\frac{\gamma_e}{\omega} \simeq -\sqrt{\frac{\pi}{2}}\frac{1}{4}\left[I_1\left(\frac{4\sqrt{7}s}{15qx_i}\right)^2\left(\frac{1}{\sigma}+\frac{1}{4}\right)+I_2q^2\frac{8}{9(1+\sigma/4)x_i^2}\right] \times\sqrt{\frac{\nu}{\omega}}\left[\ln\left(16\sqrt{\frac{\omega\epsilon}{\nu}}\right)\right]^{-3/2}. \quad (7)$$

2.3. Critical β and stability boundary

Comparing the drive, equation (2), and the damping, equations (3) and (7) and noting that $x_A = 0.226\sqrt{T_{[10\,\mathrm{keV}]}}x_i$, one can obtain a criterion for the critical β of hot particles:

$$\left(\frac{-\partial\beta_\alpha}{\partial\ln r}\right)_{\mathrm{cr}} = \frac{0.156T_{[10\,\mathrm{keV}]}^{-1/2}x_i^{-1}}{1-0.051T_{[10\,\mathrm{keV}]}x_i^2}\left\{\frac{\sigma x_i^3}{2\sqrt{2}}\frac{\mathrm{e}^{-x_i^2}}{1+\sigma/4}\right. +x_i^{-2}\sqrt{\frac{\nu}{\omega[\ln(16\sqrt{\omega\epsilon/\nu})]^3}} \left.\times\left[\frac{14}{25}\frac{I_1s^2}{q^4}\left(\frac{1}{\sigma}+\frac{1}{4}\right)+\frac{I_2}{1+\sigma/4}\right]\right\}. \quad (8)$$

Note, that in equation (8) ion Landau damping term depends only on temperature and plasma β.

It is useful to plot the stability diagrams in terms of a machine's operating parameters. In order to accomplish this we express the α-particle pressure gradient as a function of plasma β and temperature:

$$\frac{\beta_\alpha}{\beta_{\mathrm{pc}}} = \frac{8n_Dn_T}{n_e^2(1+\sigma)}\frac{\langle\sigma v\rangle n_e\tau_{\mathrm{se}}\mathcal{E}_{\alpha 0}}{12T} = \frac{\sigma^2}{1+\sigma}0.117T_{[10\,\mathrm{keV}]}^{5/2}, \quad (9)$$

where we approximated the fusion source as $\langle\sigma v\rangle \simeq 10^{-16}T_{[10\,\mathrm{keV}]}^2\,\mathrm{cm^3\,s^{-1}}$, (this expression is accurate within the range $0.7 < T_{[10\,\mathrm{keV}]} < 2$), and the energy slowing down time, τ_{se}, through $n_e\tau_{\mathrm{se}} = 2\times10^{13}T_{[10\,\mathrm{keV}]}^{3/2}\,\mathrm{cm^{-3}s}$. This formula gives the following self-consistent estimate of the α-particle pressure gradient in a self-BP:

$$\frac{-\partial\beta_\alpha}{\partial\ln r} \simeq \frac{7}{2}\beta_\alpha\frac{-\partial\ln T}{\partial\ln r} \simeq 0.0456\frac{\sigma^2}{(1+\sigma/4)x_i^2}T_{[10\,\mathrm{keV}]}^{5/2}\frac{-\partial\ln T}{\partial\ln r}. \quad (10)$$

In contrast to this expression, in present experiments the fast particle pressure gradient relies on the externally applied deposition of the neutral beam or ICRH power.

By combining equations (8) and (10) there results an equation that connects primarily three tokamak plasma parameters: $\eta \equiv -\partial\ln T/\partial\ln r$, T, and β_{pc}. Analysis shows that if ϵ, q, s, σ are similar in the machines being considered, then the plasma parametric variation for different BPs comes primarily from the parameter RB^2. Fortuitously, this parameter happens to be nearly the same for all the BP proposals considered. If we assume that the temperature profiles are parabolic $T = T_0(1-\Phi/\Phi_0)$, where $\Phi = (r/a)^2\Phi_0$ is the toroidal magnetic flux and Φ_0 is its value at the plasma edge, and r is the 'averaged' minor radius of magnetic surface, we can express the local temperature and β-values in terms of η as,

$$T = \frac{T_0}{1+\eta/2}, \qquad \beta_{\mathrm{pc}} = \frac{\beta_{\mathrm{pc0}}}{1+\eta/2}.$$

Note, that in this case the averaged temperature is $\langle T\rangle = 3T(\eta=1)/4 = T_0/2$.

With the assumption of a parabolic temperature profile and with the fusion α-particle β-value determined by equation (10) (which over-estimates the α-particle pressure as the plasma edge) one can show that since $\eta \to \infty$ at the edge (and $-\partial\beta_\alpha/\partial\ln r \to \infty$ and the growth rate $\gamma_\alpha \to \infty$), we obtain an expression where there is always such a minor radius beyond which TAEs are unstable. Figure 1 shows the critical magnetic surface minor radius $(r/a)_{\mathrm{cr}}$ above which the TAEs are unstable for different temperatures of the plasma ions $T_0 = 20, 15, 12, 10\,\mathrm{keV}$ and two different depletion factors for $\sigma = 0.8$ and 1. For depletion $\sigma = 0.8$ TAEs are stable at $T_0 = 10\,\mathrm{keV}$, which corresponds to IGNITOR parameters. However, we should note, that our model is breaking down near the edge as α-particle reaction rate, equation (9), is too large at $T_i < 7\,\mathrm{keV}$ and the collisional terms should take on a different form as well. In principle, as we approach the edge stability will arise again but it is not seen in the analytical formulation due to defects of our model in overestimating α-particle production at low temperature.

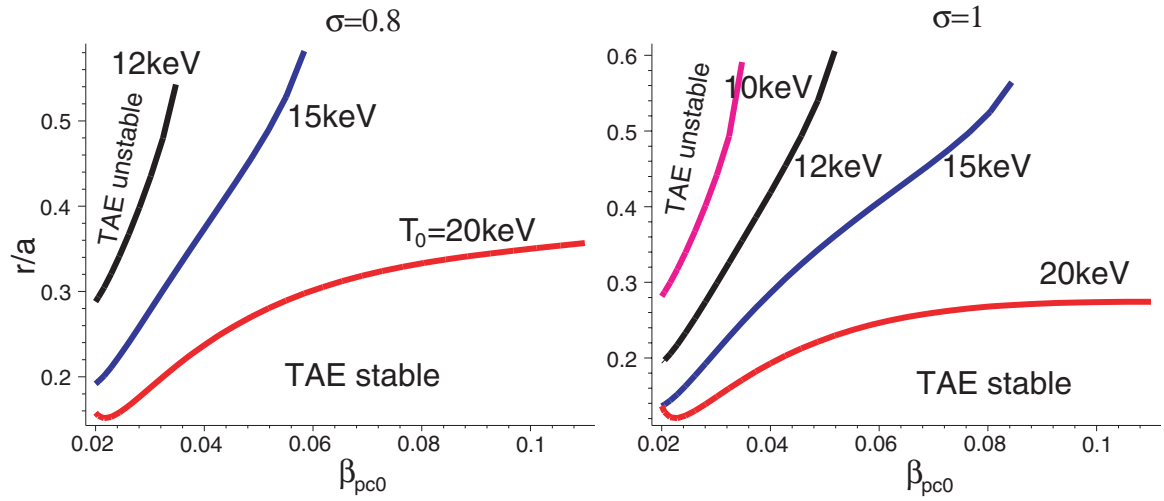

Figure 1. Critical r/a curves at which the instability is marginal for different temperatures of the plasma ions $T_0 = 20, 15, 12, 10\,\mathrm{keV}$ with fixed parabolic temperature and β-profiles of the background plasma. On the left plotted are results for $\sigma = 0.8$ and on the right for $\sigma = 1$.

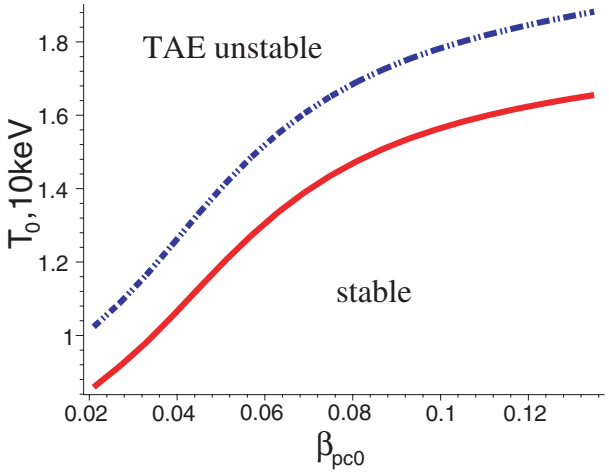

Figure 2. The stability diagram in the temperature—plasma β plane for $\eta = 1$ and depletion factors $\sigma = 1$ (——), $\sigma = 0.8$ (— · · —) is similar for three BP proposals being considered.

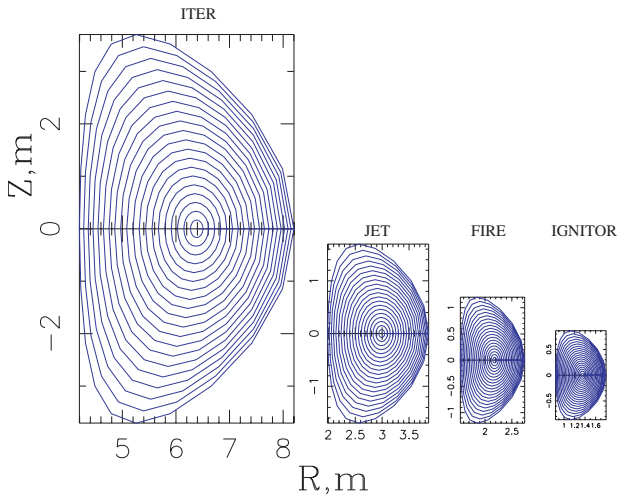

Figure 3. Plasma poloidal cross sections with magnetic surfaces of the four tokamaks under the investigation: FIRE, ITER, IGNITOR, and JET [36]. Relative sizes of these machines are compared as shown.

Equations (8) and (10) result in a transcendental equation for T as a function of plasma β. It can be solved numerically, and the results are presented in figure 2, where the TAE unstable region lies above each curve. Here, we fixed $\eta = 1$, i.e. $r/a = 1/\sqrt{3} \simeq 0.58$, which are the parameters we typically find for the most unstable surface. In plotting this and previous figures we fixed $\epsilon = a/2R$, $q = 1.5$, $s = 1$. As we mentioned for all the machines, ITER, FIRE and IGNITOR, the stability, $T(\beta_{pc})$, diagram in figure 2 looks nearly the same, so that we have shown only the diagram with FIRE parameters.

3. HINST modelling of TAE instability

In this section, we numerically explore the stability of TAE modes in the four different plasma experiments under the consideration. We use the TRANSP analysis code [34] to obtain appropriate profile parameters that are suitable for these tokamaks. In this study, we employ the non-perturbative fully kinetic code HINST [10], which solves the ballooning equation of the electromagnetic plasma oscillations. Such equation includes the toroidal coupling effects and reproduces the TAE branch [1]. This code has recently been improved to account for finite orbit orbit and realistic geometry effects. In HINST use is made of the efficient numerical equilibrium code ESC [35]. HINST shows typical agreement, to within 20%, with the growth rate calculations of core localized modes in the NOVA/NOVA-K codes. We will also compare the HINST results with our analytic estimates.

Figure 3 shows the cross sections of four devices being considered. The plasma parameters of these tokamaks are given in table 1. In the estimates of the maximum toroidal mode numbers we used equation (1) and we took for all the machines $r/aq^2 = 0.5$. A more detailed discussion of appropriate plasma parameters in BPs is published in [34]. We use the results found in that reference to establish the plasma parameter profiles for the cases reported here. The profile variations are shown in figures 4–8 as a function of $\sqrt{\Phi/\Phi_0}$. In addition, we will present the result for a 'model' q-profile, $q = 1+2.8(\Phi/\Phi_0)^{3/2}$, which is used to obtain the TAE stability criteria with a common shear profile in all the machines being considered here.

3.1. Fusion ignition research experiment

We report a detailed study of the stability results for FIRE. Figure 9 shows the comparison of the analytical damping rate with the TAE damping rate calculated by the HINST code without fast particles as minor radius dependencies. Here and later all frequencies are normalized to the central Alfvén frequency $\omega_{A0} = v_{A0}/q_0R_0$. The analytical damping rate includes ion Landau, equation (3), and trapped electron collisional damping, equation (7), that we discussed previously. In addition, we have also considered a more complicated expression for radiation damping which in [25, 21]. The results of the HINST code are in reasonable agreement with the analytical predictions within the radii $0.35 < \sqrt{\Phi/\Phi_0} < 0.5$, where the analytical formula are within its regime of applicability. The expression for the radiative damping [25] was obtained by solving analytically the system of toroidal coupled equations for TAE modes in real space whereas HINST solves numerically the eigenmode equation in ballooning poloidal angle variable. However, the same physical mechanisms are retained.

Closer to the edge, $\sqrt{\Phi/\Phi_0} > 0.5$, trapped electron collisional damping is the strongest damping mechanism, since the temperature decreases faster than the density, so that the collisional frequency increases with minor radius. In the typical instability region, $\sqrt{\Phi/\Phi_0} \sim 0.5$, ion Landau and trapped electron collisional damping are typically the two competing mechanisms. Near the plasma centre, the frequency of the core localized TAEs approaches the lower continuum and the analytical formula for radiation damping may not be valid although the detailed comparison of the analytic calculation with the HINST code appears quite good for the FIRE calculation. Note that as analytical ion Landau damping plus electron collisional damping gives a damping rate that is within a factor of two of the total damping calculated

Table 1. Main plasma parameters for tokamaks under consideration.

Tokamak	R (m)	a (m)	B_0 (T)	n_{e0} (10^{14} cm^{-3})	T_{i0} (keV)	σ	$\beta_{\alpha 0}$ (%)	$-R\nabla\beta_\alpha$ (%)	v_f/v_{A0}	v_A (10^9 cm s^{-1})	$a/\rho_{\alpha 0}$	$n_{\max}$
ITER-FEAT	6.2	2	5.3	1	19.3	0.78	0.7	5	1.8	0.72	39.1	10
FIRE	2.14	0.6	10	4.9	11.9	0.825	0.28	1.3	2.1	0.62	22.14	5
IGNITOR	1.32	0.48	13.1	9.4	9.9	0.91	0.2	0.8	2.21	0.59	23.2	5
JET-DT	2.92	0.94	3.82	0.45	23	0.795	0.4	2.3	1.66	0.78	13.25	4

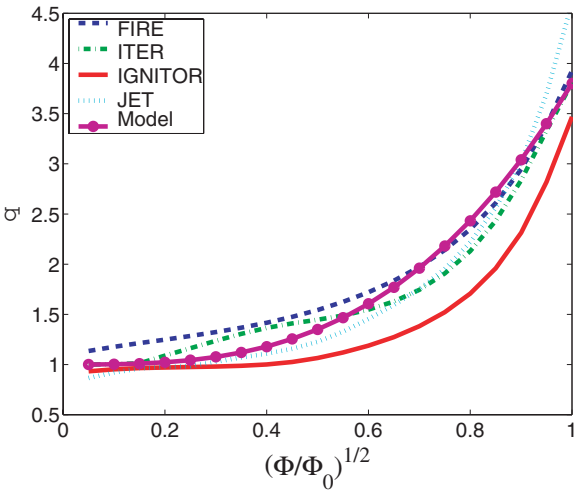

Figure 4. Safety factor profiles for the four machines under consideration and the 'model' q-profile used in HINST calculations.

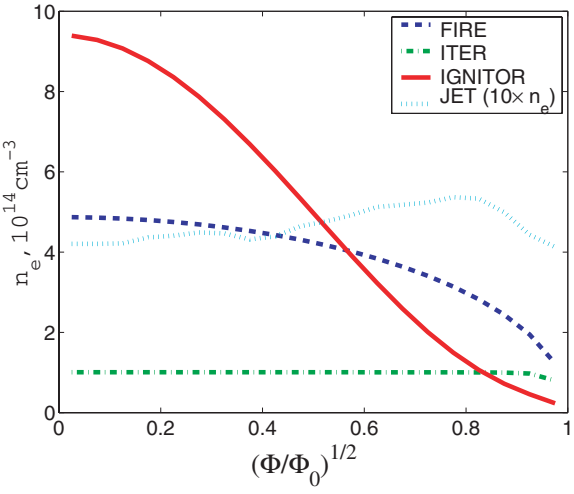

Figure 6. Electron density profiles for the four machines under consideration.

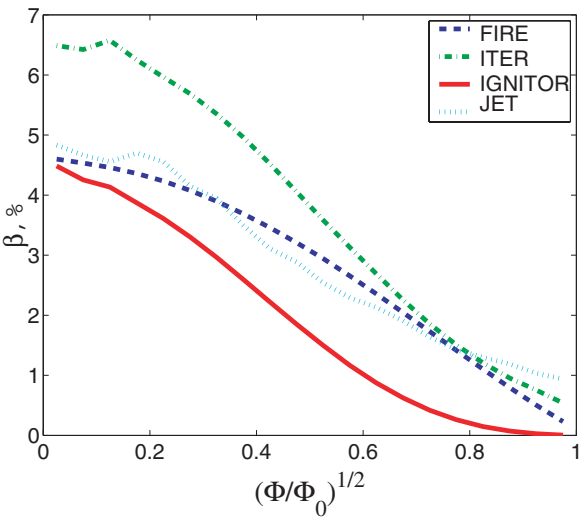

Figure 5. Total plasma β-profiles for the four machines under the consideration.

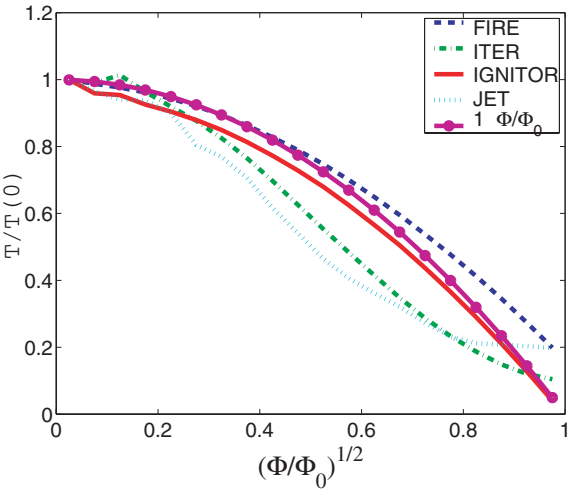

Figure 7. Normalized temperature profiles for the four machines under consideration compared with the parabolic profile.

in HINST (see also damping calculations for ITER later) the analytical expression used in the previous section appears to be a reasonable approximation for the total damping.

For the TAE instability calculations we use the TRANSP computed plasma core and α-particle β-profiles that are shown in figures 5 and 8. The results from the HINST code for the nominal FIRE plasma are shown in figure 10 in the form of the eigenfrequency and the growth rate for TAEs as functions of $\sqrt{\Phi/\Phi_0}$, where the TRANSP generated q-profile was used. The comparison of the instability using the aforementioned model q-profile, but otherwise parameters obtained from TRANSP, is shown in figure 11 for FIRE for the $n = 7$ mode number. Figure 12 (FIRE curves with the model q-profile) shows the eigenfrequency and growth rate computed by the HINST code for different toroidal mode numbers on the surface with the highest growth rate.

With the TRANSP calculated central value of $\beta_{\alpha 0} = 0.28\%$, the radial span of the TAE unstable region lies within $0.5 < \sqrt{\Phi/\Phi_0} < 0.65$ and the growth rate sharply decreases outside that region. Since the solutions of TAEs

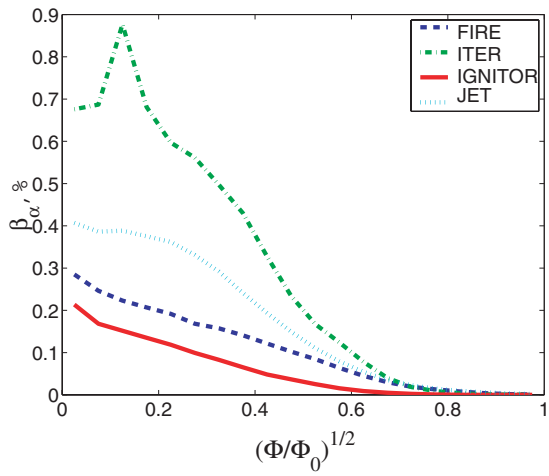

Figure 8. α-particle β-profile for four considered devices.

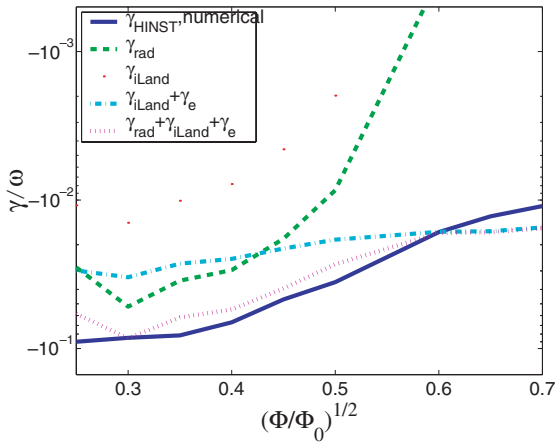

Figure 9. Comparison of numerical damping rates from HINST code with the analytical ones in FIRE for the $n = 10$ TAE mode.

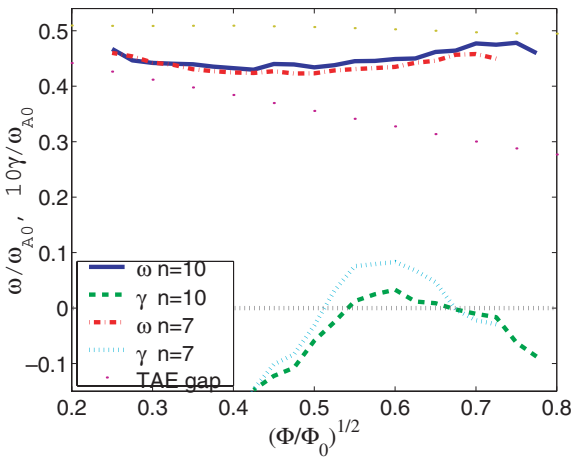

Figure 10. TAE eigenfrequency and growth rate as functions of minor radius variable $\sqrt{\Phi/\Phi_0}$ in FIRE with TRANSP q-profile for $n = 7$ and 10.

typically have a global structure, a more accurate calculation for the stability will require taking an appropriate average over a large portion of the minor radius. Thus, the final question of establishing a TAE critical β requires a global calculation. The

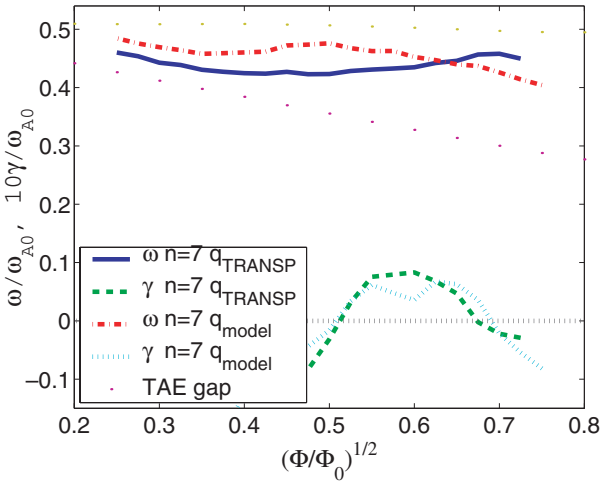

Figure 11. Comparison of TAE eigenfrequency and growth rates as functions of minor radius in FIRE for TRANSP and model q-profiles at fixed $n = 7$.

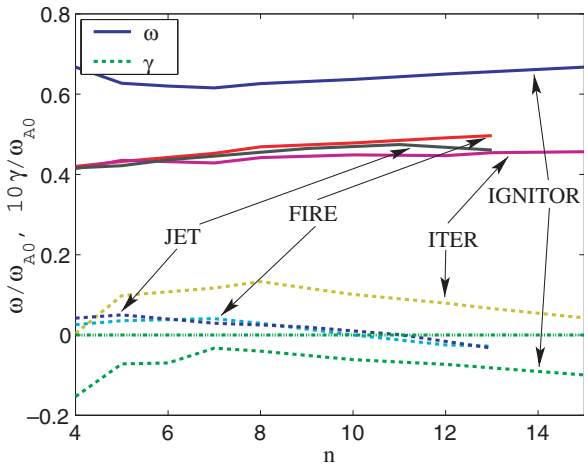

Figure 12. Eigenfrequency and growth rate of TAE vs toroidal mode number computed by the HINST with the model q-profile and a fusion α-particle drive for the four tokamaks being studied.

HINST code can in principle be improved to take into account the spatial extent of a mode, but the code is not yet ready to study this case. Such a non-local calculation can be performed with the NOVA/NOVA-K codes. The resulting stability predictions are described in the next section. However, global calculations with NOVA/NOVA-K codes are perturbative with some physical effects ignored, such as stronger mode coupling through plasma shaping, and, thus, stronger continuum damping [37]. We point out that these approximations and omissions introduce another set of uncertainties in the NOVA-K calculations. For example, the perturbation theory presently used does not account for any possible mode structure changes induced by strong drive and damping mechanisms that peak in different spatial regions. A more sophisticated perturbation theory may in turn result in instability arising from TAE localization around a region of strong drive.

The instability becomes stronger if at a fixed plasma β the temperature is increased and correspondingly the density is lowered. In the following example we keep the same temperature and density profiles as in the previous study but we

change only the central values of following plasma parameters $n_{e0} = 3.65 \times 10^{14}\,\mathrm{cm}^{-3}$, $\beta_{\mathrm{pc}0} = 5.6\%$, $\beta_{\alpha 0} = 1.1\%$, $T_{i0} = 21.4\,\mathrm{keV}$ and used the model q-profile. Results are shown in figure 13.

3.2. *International tokamak experimental reactor*

We performed similar TAE instability growth rate calculations for an ITER plasma. The numerical q-profile that emerges from TRANSP is not smooth due to several factors, such as NBI and ICRH heating. We performed the calculations of the damping rates for the model q-profile shown in figure 4. Figure 14 shows the comparison of TAE analytical damping rates (same as in FIRE study, section 3.1) with the damping rate found in the HINST code without α-particles.

Figures 15 and 12 (ITER curves) represent the eigenfrequency and the growth rate of TAEs computed by the HINST code as functions of $\sqrt{\Phi/\Phi_0}$ and toroidal mode number n, respectively. As expected from our estimates in table 1 the maximum growth rate for ITER in the local calculations is shifted to higher $n \simeq 9$. In ITER, the instability region is shifted toward smaller minor radii, which is primarily due to the lower damping that is present at $\sqrt{\Phi/\Phi_0} \sim 0.5$.

In ITER there are plans to use NBI heating (injected in the direction of plasma current). In order for neutral beam particles to penetrate into the plasma, high energy beams have to be used. At the planned injection energy, $\mathcal{E}_{b0} = 1\,\mathrm{MeV}$, the energetic particles created by the beams make a significant additional contribution to the drive of TAEs for a wide range of n-values due to the large value of $\omega_{*\alpha}$ term and as a consequence of a strong anisotropy in velocity space of the beam ion distribution function. We will defer the study of the effect of beams to the next section where the NOVA calculations are reported.

3.3. *IGNITOR*

Figure 16 and 12 (IGNITOR curves) represent the eigenfrequency and the growth rate of TAEs computed by the HINST code as functions of $\sqrt{\Phi/\Phi_0}$ and toroidal mode number n, respectively. TAEs turn out to be robustly stable

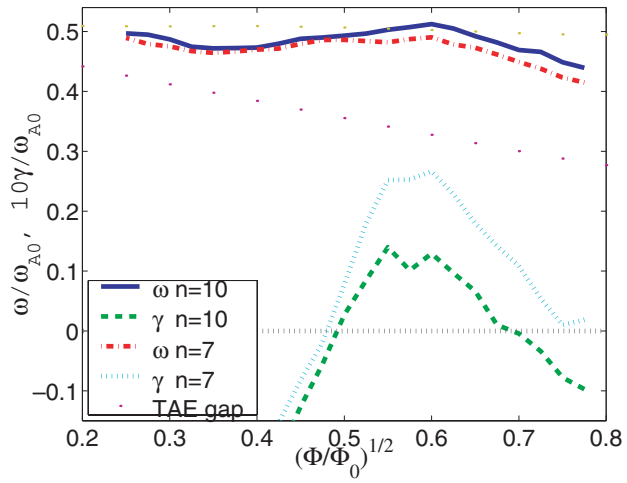

Figure 13. TAE eigenfrequency and growth rate as functions of minor radius in FIRE with model q-profile at higher plasma temperature ($T_0 = 21.4\,\mathrm{keV}$).

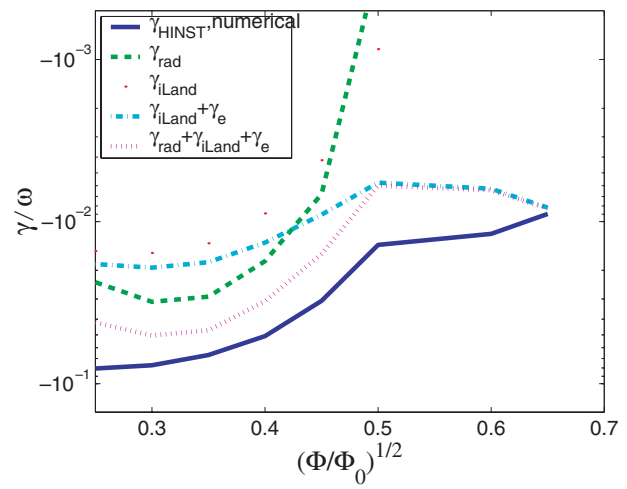

Figure 14. Comparison of numerical damping rates from HINST code with the analytical damping (same as in section 3.1) rates in ITER for $n = 10$ TAE.

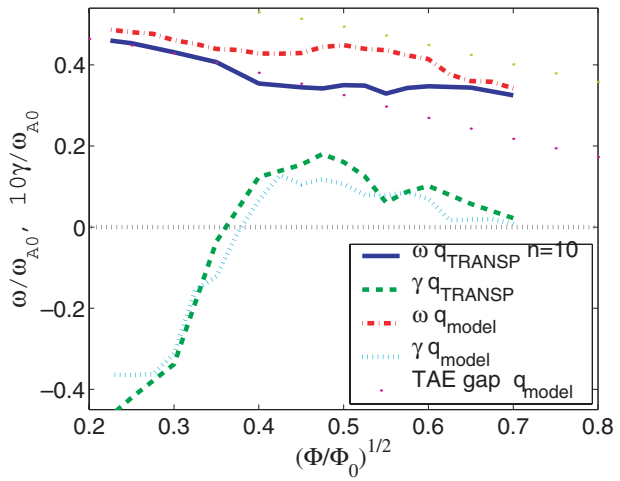

Figure 15. TAE eigenfrequency and growth rate as functions of the minor radius in ITER for model and TRANSP q-profiles.

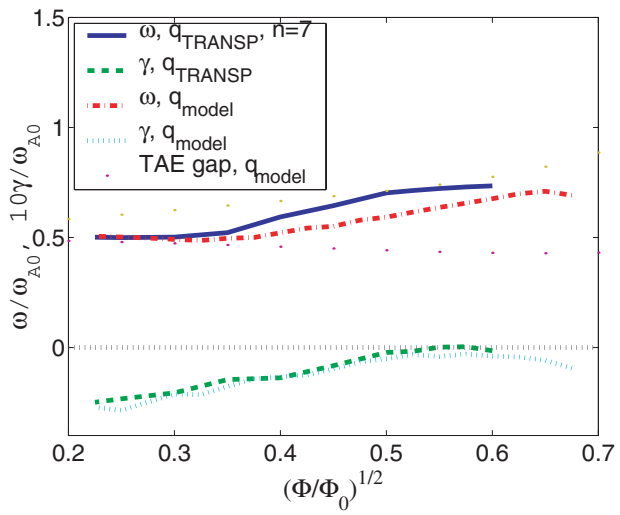

Figure 16. TAE eigenfrequency and growth rate as functions of minor radius in IGNITOR.

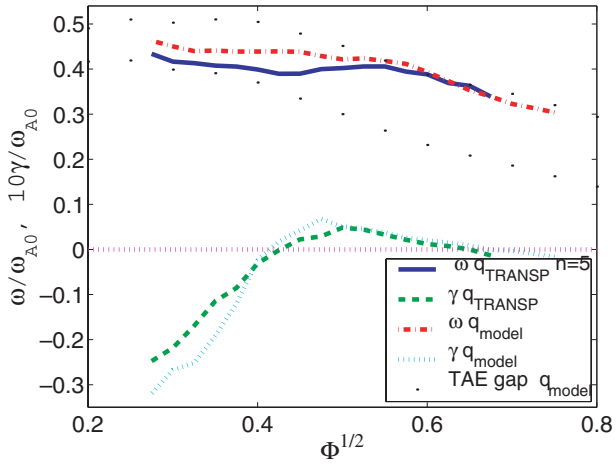

Figure 17. TAE eigenfrequency and growth rate as functions of minor radius in the JET D–T plasma.

in IGNITOR, though sometimes close to the point of marginal stability. The stability is due to a low α-particle β that is a consequence of the lower plasma temperature than in the other BP proposals. This leads to strong collisional damping on trapped electrons and a weaker drive. Global calculations are expected to gives even stronger damping of TAEs.

3.4. JET

As an attempt to connect our numerical predictions with the existing experiments we analyse a JET D–T plasma [36]. Figures 17 and 12 (JET curves) represent the eigenfrequency and the growth rate of TAE's computed by the HINST code as functions of $\sqrt{\Phi/\Phi_0}$ and toroidal mode number n, respectively. The maximum growth rate in JET, without beams, is rather low and is expected to be at $n \simeq 6$, which is close to what was predicted in other studies [38, 22]. However with the NBI heating that was used, an additional strong stabilizing effect is present. We computed the TAE growth rate for an NBI β $\beta_b(0) = 0.6\%$ at an injection energy of deuterium $\mathcal{E}_{b0} = 100$ keV. The calculations show that without fast particles the eigenfrequency at $\sqrt{\Phi/\Phi_0} = 0.5$ and $n = 5$, is $\omega/\omega_{A0} = 0.395 - \mathrm{i}9 \times 10^{-4}$. With α-particles (no beams) we obtain $\omega/\omega_{A0} = 0.402 + \mathrm{i}4.8 \times 10^{-3}$. With isotropic passing beam ions (no αs and isotropic beams are used as at the moment the HINST code does not properly treat anisotropic beams) we obtain $\omega/\omega_{A0} = 0.42 - \mathrm{i}1.1 \times 10^{-2}$. If we add the partial contributions to the growth rate from NBI ions and αs we find that the TAEs should be stable primarily due to damping on beam ions. This conclusion is consistent with the study in [38, 22]. As was expected in JET the number of unstable modes is less than for the BP proposals $\leqslant 7$ (see figure 12). This is also true for the excitation of TAEs in D–T experiments in TFTR [27].

4. NOVA modelling of TAE instability

One of the advantages of using the HINST code is in its rapid calculational ability. This allows us to focus our study in NOVA, a more time consuming code for investigating the most unstable high-n cases. NOVA modelling is based on a set of codes, which includes the ideal MHD computation of TAE eigenmodes [39] and the perturbative NOVAK post-processing of the different driving and damping mechanisms. The perturbative effects include: the fast particle pressure gradient drive with finite orbit width (FOW) and FLR effects, background ion and electron Landau damping, trapped electron collisional damping and radiation damping which is accurate in a limited perturbation region [39, 21, 31]. In this paper, we report the NOVAK study of ITER and FIRE with the plasma parameters provided by TRANSP. We omit reports of a study of IGNITOR and JET because they are stable in the local calculations we have previously discussed. The global studies of these latter two machines are not expected to introduce any de-stabilization of TAEs.

In the nominal ITER experiment it is planned that the core region will include fast particles arising from 1 MeV neutral beam injection for the purpose of heating and current drive. To asses this effect from neutral beams we take a distribution function that is peaked with velocities nearly parallel to the field line with the particle moving along the direction of plasma current. We assume the beam has a spread in pitch angle that is larger than the mean pitch angle of the beam. Thus, we take a slowing down distribution, multiplied by a weighting factor

$$f_\lambda(\lambda) = \mathrm{e}^{-\lambda^2/\Delta_\lambda^2} \frac{4}{\Delta_\lambda \sqrt{\pi}},$$

where $\lambda = v_\perp^2 / B v^2$. Under our assumptions it can be shown that the width $\Delta\lambda$ produces anisotropy with a mode growth rate that is independent of $\Delta\lambda$. Further, the Landau damping term due to fast beam ions is approximately reduced by a factor of 3.

The following figures summarize this study for ITER, figure 18, and FIRE, figure 19. In addition to TAEs, we analysed ellipticity (EAE) and triangularity (NAE) induced modes. However, in its present version NOVAK computes radiation damping only for modes with eigenfrequincies inside the TAE gap. In the nominal ITER proposal these modes are also unstable. However, most of these modes interact with the continuum and if their structure is extended radially they may be stabilized by the continuum interaction that is not included in the NOVA calculation. Some of the modes have localized radial structure. One example of such modes is shown in figure 21 (right). We observe that it is localized well inside the gap, so that the mode can be expected to only weakly interact with the continuum. In general, the stabilization by the continuum will depend on the shape of the gap.

One can see from figure 18 that the presence of beam ions expands the spectrum of unstable modes toward higher n-values and that the contribution to the AE drive from beam ions is of the same order as the α-particle drive. To attempt to reduce the beam ion contribution to the growth rate one can investigate whether beams with smaller injection speed than the Alfvén speed, would produce significantly less de-stabilization, such beam ions may not interact with the strongest resonance at the Alfvén speed. Instead, the primary interaction would be a speed that is equal to a third of the Alfvén speed. We performed special calculations to study whether such beams with energy $\mathcal{E}_{b0} < 540$ keV can be deposited sufficiently deep into the plasma. The TRANSP code simulations indicate that at $\mathcal{E}_{b0} = 500$ keV the beam deposition profiles will still be peaked at the centre,

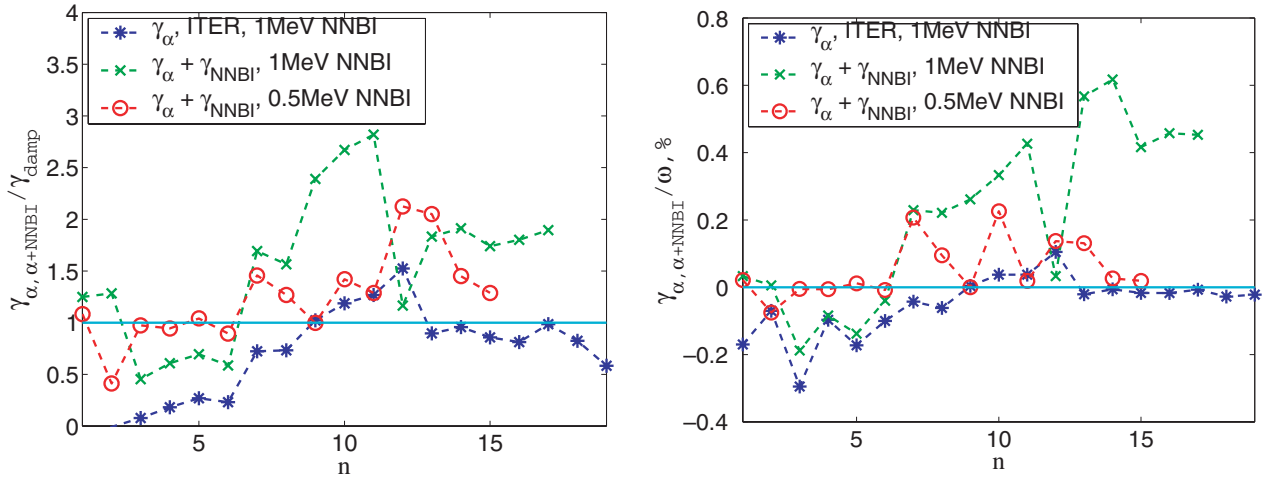

Figure 18. NOVAK results of the AE growth rates for ITER. Shown on the left are the maximum ratio of drive to damping for the cases where there is drive from α-particles alone and when the drive is from both α-particles plus 1 MeV neutral beams. Plotted on the right is the maximum total growth rate of the modes with and without beams. Both figures are plotted as functions of the mode toroidal number n.

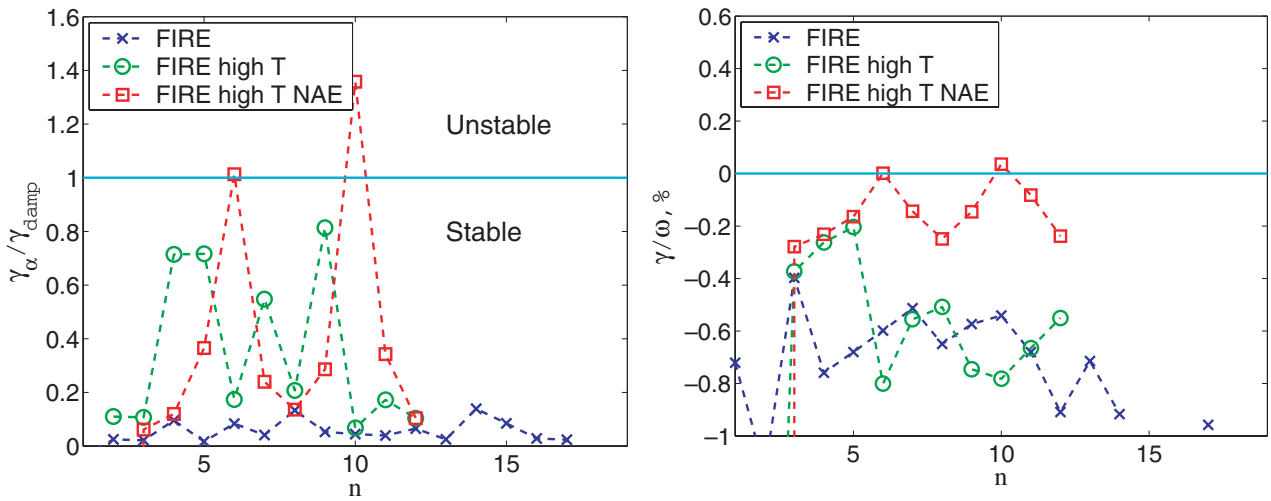

Figure 19. NOVAK calculations of TAE, EAE and NAE growth rates for FIRE. Shown are the maximum (among different modes for each n) ratio of the α-particle drive to the damping (left) and the total growth rate of the modes versus the mode toroidal number n for the nominal and elevated temperature profiles discussed in section 3.1.

while at $\mathcal{E}_{b0} = 280\,\text{keV}$ the injected beam neutrals will be confined with the hollow pressure profile. NBI β-profiles for injection energies $\mathcal{E}_{b0} = 1\,\text{MeV}$, 500 keV, 280 keV are shown in figure 20. The NOVA calculations show (see figure 18) that with a lower injection beam energy of $\mathcal{E}_{b0} = 500\,\text{keV}$ that there is a stabilizing effect on TAEs when compared to the 1 MeV case, even though the 500 keV case is destabilizing compared with a system without beams. However, note that with 500 keV beams, the stable modes at low n ($3 \leqslant n \leqslant 6$) are more destabilizing for the 500 keV beam case than for the 1 MeV beam case. We see that in this lower n-regime the TAEs are marginally stable for the 500 keV case, whereas this regime was stable for 1 MeV beams. Further decrease of NBI injection energy to below $\mathcal{E}_{b0} < 500\,\text{keV}$ may limit the performance of the ITER design as shown in figure 20.

In figure 19, we show the stability results for FIRE. The NOVA study of the FIRE nominal case shows that

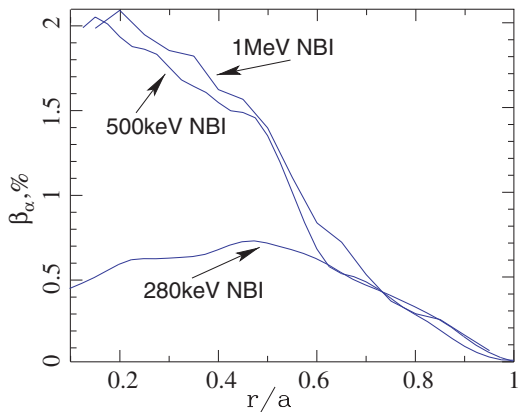

Figure 20. NBI β-profiles for different injection energies $\mathcal{E}_{b0} = 1\,\text{MeV}$, 500 keV, 280 keV with the same power $P_b = 33\,\text{MW}$ in ITER as predicted by TRANSP.

all AEs are stable for the low temperature case which was outlined in section 3. However, for the high temperature case TAEs and EAEs are marginally stable, while NAEs show instability. These modes are localized near the core. The NAEs have substantially less ion Landau damping than the TAEs. In large aspect ratio theory, ion Landau damping of TAEs comes primarily from the sideband at the parallel speed, $v_\parallel = v_A/3$, whereas for the NAE the sideband lowest velocity is $v_\parallel = 3v_A/5$. Since, the population of resonant particles is proportional to a Maxwellian tail, $e^{m_i v_\parallel^2/2T_i}$, ion Landau damping from an NAE is strongly reduced. The growth rate for NAEs is also small. In previous experiments it was pointed out that NAEs have the lowest excitation threshold when ICRH was applied [40]. There were no measurements of the effects of NAEs excitation on fast particle confinement in those experiments.

4.1. Global versus local analysis in NOVAK

As we pointed out the global mode structure predicted by the NOVA code provides more stabilization than in the HINST local code. This is because for the global mode, the stabilization is weighted from the mode structure near the outer edge of the plasma while destabilization is driven be the mode structure in the central region where the α-particle (and perhaps beam) drive is strong. For high-n one can find modes with the same n-value where the frequency difference is less than the imaginary frequency shifts arising from damping or growth. To treat such a case properly requires the use of a degenerate perturbation theory, where the damping and growth mechanisms allow different modes with the same n-value to interact, and possibly produce a different mode structure as the near degeneracy of the lowest order modes are resolved. Thus, there is therefore concern that the perturbative NOVAK analysis, that excludes modes of the same n-value from interacting with each other, can be inaccurate. In particular, it may be possible for modes to form that are localized to the interior, where α drive dominates local dissipative mechanisms (such modes would be substantially more unstable than the present calculations from NOVAK) and modes that localize in the external region, where edge collisional dissipation is dominant (such modes would be more stabilizing than present NOVAK predictions). To place an upper bound on the instability prediction that might emerge from a more accurate perturbative analysis code, we use the NOVAK code by just calculating the drive and damping for a single TAE couplet where the mode peaks. We performed a special study of this effect in ITER and FIRE. In figure 21, we show the eigenmodes of the TAE branch for FIRE, $n = 7$ and ITER, $n = 10$. Shown as dash-dotted lines are harmonics used in such pessimistic NOVAK stability analysis. Table 2 summarizes this study. For ITER and FIRE the local mode structure produces unstable

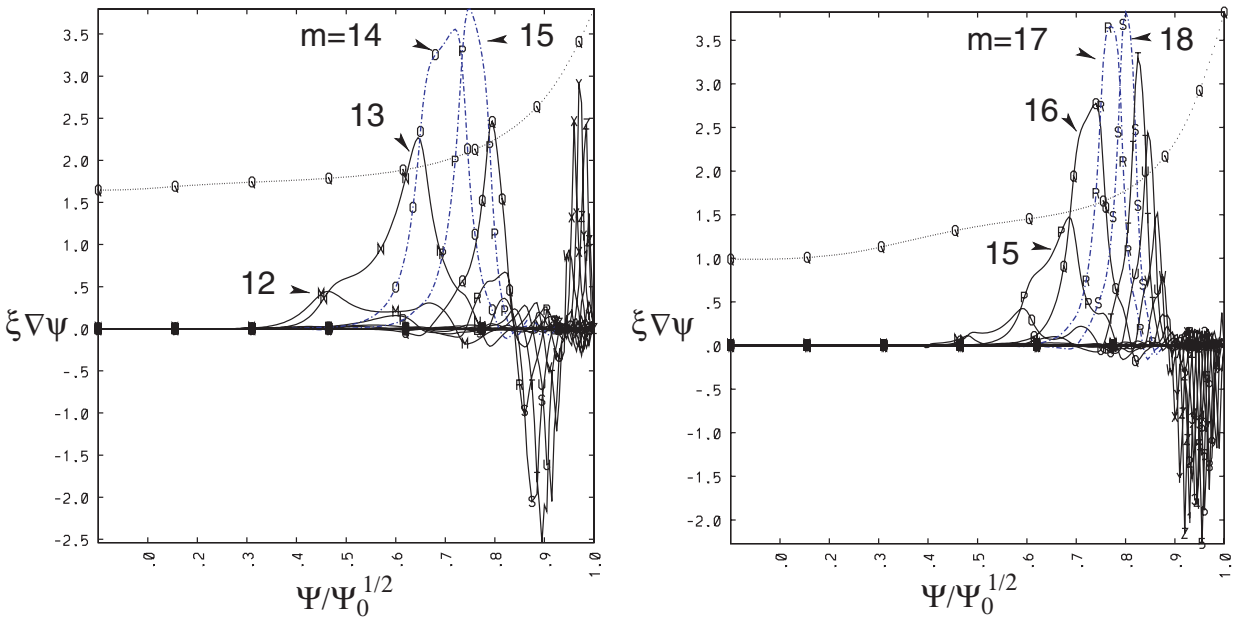

Figure 21. Eigenmode structure of TAEs in FIRE, $n = 7$ (left) and ITER, $n = 10$ (right). Shown as dash-dotted lines are harmonics used in 'local' (more pessimistic for the stability) NOVAK analysis, in which all other harmonics were excluded.

Table 2. The comparative results for global and 'local' NOVA cases (when only two dominant harmonics are kept) for the growth and damping rate calculations for the FIRE high temperature case and ITER.

	$\frac{\gamma_\alpha}{\omega}$ (%)	$\frac{\gamma_b}{\omega}$ (%)	$\frac{\gamma_{\rm rad}}{\omega}$ (%)	$\frac{\gamma_e}{\omega}$ (%)	$\frac{\gamma_{eL}}{\omega}$ (%)	$\frac{\gamma_{D\rm Land}}{\omega}$ (%)	$\frac{\gamma_{T\rm Land}}{\omega}$ (%)	$\frac{\gamma_\Sigma}{\omega}$ (%)	$\left(\frac{\omega q_a}{\omega_{A0}}\right)^2$
FIRE, $n = 7$	2.26		−3.4	−26.5	−0.1	−0.9	−0.5	−29	0.68
FIRE, pessimistic	8.9		−2.53	−0.9	−0.2	−2.45	−1.6	1.2	0.68
ITER, $n = 10$	0.29	0.36	−0.09	−0.27	−0.2	−0.1	−0.05	−0.06	1.21
ITER, pessimistic	1.28	0.88	−0.12	−0.14	−0.2	−0.43	−0.26	1	1.21

modes. In FIRE, particularly for the high temperature case, the growth rate for the local mode is very strong up to $\gamma/\omega \sim 10\%$. Such a large value is perhaps indicative that even a perturbative approach in NOVA calculations may not be justifiable and the high temperature FIRE scenario could be susceptible to the non-perturbative so-called resonance TAEs [11] or EPMs [12–14]. This issue needs to be addressed in future studies.

5. Conclusions

Analyses of stability have been performed by three independent methods: analytical, numerical using the local kinetic non-perturbative HINST code, and numerical using the global code NOVA. These studies show that Alfvén modes should be robustly stable in IGNITOR, due to the lower fast particle β and relatively strong collisionality which produces significant trapped electron collisional damping. Analytical and HINST calculations predict TAE instability in FIRE and ITER. The global perturbative code NOVA predicts TAEs in ITER to be slightly unstable. However, when instability is predicted there may be a significant stabilizing contribution from the continuum that has not been accounted for. We have noted that in ITER NBI at 1 MeV strongly contributes to the TAE instability drive with a growth rate comparable to the one due to fusion αs. To make beam ions stabilize one should decrease their energy below 540 keV, so as to minimize the effect of the direct principal resonance with TAEs. NBI with such injection energy need to satisfy the requirement of penetration into the core of the plasma. At $\mathcal{E}_{b0} = 540\,\mathrm{keV}$ beam ions still drive the TAE unstable, but compared with the 1 MeV neutral beam injection case, the growth rate of unstable modes is significantly reduced.

For the high temperature FIRE scenario, NOVA predicts instability due to NAE's. At somewhat higher temperature, $T_{i0} = 21.4\,\mathrm{keV}$, TAEs are marginally stable in FIRE. Our study raises the issue of whether the TAE perturbative analysis has been properly applied for ITER and the high temperature FIRE case. It may be possible that spatially localized interactions can break-up the large global extent of the modes. Then the dominant larger damping arising near the plasma edge would not be as effective as it currently is in the perturbative NOVAK analysis to produce stabilization. Indeed, since the modes occur at high-n, where many eigenmodes have frequencies close to each other, it may be possible for an unstable mode to localize in the core when a more sophisticated analysis is used.

Acknowledgments

This work was supported by the United States Department of Energy under Contract Nos DE-AC02-76CH03073 and DE-FG03-96ER-54346.

References

[1] Cheng C.Z., Chen L. and Chance M.S. 1985 *Ann. Phys.* **161** 21
[2] Cheng C.Z. and Chance M.S. 1986 *Phys. Fluids* **29** 3695
[3] Cheng C.Z., Fu G.Y. and Van Dam J.W. 1988 *Princeton Plasma Physics Laboratory Report* PPPL-2585 (January 1989) p 14 *Proc. Joint Varrena-Lausanne Workshop on Theory of Fusion Plasmas (Lausanne, Switzerland, 3–7 October 1988)* pp 259–70
[4] Fu G.Y. and Van Dam J.W. 1989 *Phys. Fluids* B **1** 1949
[5] Wong K.L. 1997 *Plasma Phys. Control. Fusion* **39** 2471
[6] Heidbrink W.W. and Sadler G.J. 1994 *Nucl. Fusion* **34** 535
[7] Campbell D.J. 2001 *Phys. Plasmas* **8** 2041
[8] Meade D. 2000 *Com. Plasma Phys. Control. Fusion, Com. Modern Phys.* **2** 81
[9] Coppi B. *et al* 2001 *Nucl. Fusion* **41** 1253
[10] Gorelenkov N.N., Cheng C.Z. and Tang W.M. 1998 *Phys. Plasmas* **5** 3389
[11] Cheng C.Z., Gorelenkov N.N. and Hsu C.T. 1995 *Nucl. Fusion* **35** 1639
[12] Chen L. 1994 *Phys. Plasmas* **1** 1519
[13] Briguglio *et al* 1995 *Phys. Plasmas Control. Fusion* A **279** 37
[14] Santoro R.A. and Chen L. 1996 *Phys. Plasmas* **3** 2349
[15] Heidbrink W.W., Strait E.J., Chu M.S. and Turnbull A.D. 1993 *Phys. Rev. Lett.* **71** 855
[16] Gorelenkov N.N. and Heidbrink W.W. 2002 *Nucl. Fusion* **42** 150
[17] Heidbrink W.W., Gorelenkov N.N. and Murakami M. 2002 *Nucl. Fusion* **42** 972
[18] Bernabei S. *et al* 2001 *Nucl. Fusion* **41** 513
[19] Gorelenkov N.N. *et al* 2000 *Nucl. Fusion* **40** 1311
[20] Cheng C.Z. 1992 *Phys. Rep.* **211** 1
[21] Fu G.Y. *et al* 1996 *Phys. Plasmas* **3** 4036
[22] Borba D. *et al* 2000 *Nucl. Fusion* **40** 775
[23] Mett R.R. and Mahajan S.M. 1992 *Phys. Fluids* B **4** 2885
[24] Candy J. and Rosenbluth M.N. 1994 *Phys. Plasma* **1** 356
[25] Berk H.L., Mett R.R. and Lindberg D.M. 1993 *Phys. Fluid* B **5** 3969
[26] Fu G.Y., Nazikian R., Budny R. and Chang Z. 1998 *Phys. Plasmas* **5** 4284
[27] Nazikian R. *et al* 1997 *Phys. Rev. Lett.* **78** 2976
[28] Kramer G.J., Sharapov S.E., Nazikian R., Gorelenkov N.N., Budny R. First evidence for the existence of odd toroidal Alfvén eigenmodes (TAEs) from the simultaneous observation of even and odd TAEs on the joint European torus *PPPL Report* 3768 *Phys. Rev. Lett.* submitted
[29] Berk H.L., Breizman B.N. and Ye H. 1992 *Phys. Lett.* A 475
[30] Breizman B.N. and Sharapov S.E. 1995 *Plasma Phys. Control. Fusion* **37** 1057
[31] Gorelenkov N.N., Cheng C.Z. and Fu G.Y. 1999 *Phys. Plasmas* **7** 2802
[32] Gorelenkov N.N. and Sharapov S.E. 1992 *Phys. Scr.* **45** 163
[33] Fu G.Y. and Cheng C.Z. 1992 *Phys. Fluids* B **4** 3722
[34] Budny R.V. 2002 *Nucl. Fusion* **42** 1383
[35] Zakharov L.E. and Pletzer A. 1999 *Phys. Plasmas* **6** 4693
[36] Pamela J. *et al* 2002 *Nucl. Fusion* **42** 1014
[37] Jaun A., Fasoli A., Vaclavik J. and Villard L. 2000 *Nucl. Fusion* **40** 1343
[38] Sharapov S.E. *et al* 1999 *Nucl. Fusion* **39** 373
[39] Cheng C.Z. 1991 *Phys. Fluid* B **3**
[40] Kramer G.J., Saigusa M., Ozeki T., Kusama Y., Kimura H., Oikawa T., Tobita K., Fu G.Y. and Cheng C.Z. 1998 *Phys. Rev. Lett.* **80** 2594